International Journal of
Sensor Networks and Data Communications

Azizi et al., Int J Sens Netw Data Commun 2016, 5:4
DOI: 10.4172/2090-4886.1000149

Research Article Open Access

Bifurcation Behavior of a Capacitive Micro-Beam Suspended between Two Conductive Plates

Azizi A[1]*, Mobki H[2] and Rezazadeh G[3]

[1]Department of Engineering, German University of Technology, Halban, Oman
[2]Department of Mechanical Engineering, University of Tabriz, Iran
[3]Department of Mechanical Engineering, Urmia University, Iran

Abstract

In this paper, bifurcation and pull-in phenomena of a capacitive micro switch suspended between two stationary plates have been studied. The governing dynamic equation of the switch has been attained using Euler Bernoulli beam theorem. Due to the nonlinearity of the electrostatic force, the analytical solution for the derived equation is not available. So the governing differential equation has been solved using combined Galerkin weighted residual and Step-By-Step Linearization Methods (SSLM).

To obtain the fixed points and study the local and global bifurcational behavior of the switch, a mass-spring model has been utilized and adjusted so that to have similar static/dynamic characteristics with those of Euler-Bernoulli beam model (in the first mode). Using 1-DOF model, mathematical and physical equilibrium points of the switch have been obtained for three different cases. It is shown that the pull-in phenomenon in the present micro-switch can be occurred due to a pitchfork or transcritical bifurcations as well as saddle node bifurcation which are transpired in the classical micro-switches. And for some cases primary and secondary pull-in phenomena are observed where the first one is due to a transcritical bifurcation and the second one is due to a saddle node bifurcation. In addition the dynamic response of the switch to a step DC voltage has also been studied and the results show that in contrast to the classical micro-switches, the ratio of the dynamic pull-in to the static one depends on the gaps and voltages ratio where for the classical one is approximately a constant value.

Keywords: Electrostatic actuation; Micro-switch; Nonlinear dynamic; Transcritical bifurcation; Saddle node bifurcation

Introduction

"Bifurcation, a French word introduced into nonlinear dynamics by Poincare, is used to indicate a qualitative change in the features of a system, such as the number and type of solutions, under the variation of one or more parameters on which the considered system depends" [1]. Electro statically actuated Micro Electro Mechanical (MEM) and Nano Electro Mechanical (NEM) systems form a broad class of devices, which bifurcational behavior can be observed due to the nonlinearity of the electrostatic force.

Nowadays, because of the advantages of the electrostatic actuators, such as favorable scaling property, low driving power, large deflection capacity, relative ease of fabrication, and others, have led to their being more widely applied for electrostatic-actuator applications in MEM systems. The MEM switch is one of the most important devices in such systems. The structural elements that are used in MEM devices are typically simple elements including micro-beams, plates, and membranes. Electro statically actuated micro-beams (e.g., cantilever and fixed–fixed micro-beams) are used in many MEM devices such as capacitive MEM switches and resonant sensors. Manufacturing and design of these devices are, to some extent, in a more mature stage than those of some other MEM devices [2].

One of the most significant issues in the capacitive micro and nano switches is the pull-in instability. In these devices, a movable beam/plate is suspended over a stationary plate, and a potential difference is applied between them. As the micro-structure is balanced between two forces, namely, electrostatic (attractive) and mechanical (elastic restoring) forces, both of these forces are increased when the applied voltage increases. When the voltage reaches a critical value, pull-in instability occurs. Pull-in is a situation at which the elastic restoring force can no longer balance the electrostatic attractive force. Further increasing the voltage will cause the structure to have a sudden displacement jump, causing structural collapse and failure. Pull-in instability is a snap-through like behavior and it is a saddle-node bifurcation type of instability [3].

The pull-in phenomenon usually occurs in many micro-machine devices which require bi-stability for their operation, such as in the MEM and NEM switches [4,5]. Many studies have been developed in the analysis of instability of the MEM structures due to their nonlinearity [6,7]. Zhang and Zhao [8] studied the Pull-in instability of a MEM switch under electrostatic actuation. Taghizadeh and Mobki [9] analyzed the pull-in phenomenon of a torsional micro-mirror. In nano scale, Dequesnes et al., [10,11] and Hosseini et al., [12] investigated the static and dynamic stability of a carbon nano tube. Mobki et al., [13] studied the static and dynamic pull-in phenomenon of a capacitive nano-beam, considering length scale-parameter.

In the case of bifurcational behavior of the MEM and NEM systems, some works have been done. Lin and Zhao [14-16] studied bifurcation and pull-in phenomenon of NEM actuators with considering van der Waals (vdW) and Casimir forces. They showed that the pull-in voltage causes a saddle node type bifurcation in these devices. Many researchers

***Corresponding author:** Azizi A, Department of Engineering, German University of Technology, Oman, Tel: 96822061000; E-mail: Aydin.azizi@gutech.edu.om

Received April 28, 2016; **Accepted** December 28, 2016; **Published** January 06, 2017

Citation: Azizi A, Mobki H, Rezazadeh G (2016) Bifurcation Behavior of a Capacitive Micro-Beam Suspended between Two Conductive Plates. Int J Sens Netw Data Commun 5: 149. doi: 10.4172/2090-4886.1000149

have shown that the saddle node bifurcation, can be transpired in the electro statically MEM/NEM devices [3,9,13-18].

In spite of many research works accomplished on the stability of MEM structures, there is not enough comprehensive work explaining the stability of these switches from the type of bifurcation point of view.

In the present study, different types of bifurcation are investigated for a capacitive micro-beam suspended between two conductive plates. It should be mentioned that this specific sort of micro-switch allows us to produce different bifurcation types, by varying of some parameters. The micro-beam (micro-switch) is actuated by electrostatic forces induced by DC polarization voltages. Also, to study the bifurcation of the beam, the nonlinear equation of the dynamic motion of the Euler Bernoulli beam using a one term Galerkin weighted residual method is converted to a lumped mass-spring model. Compared to the distributed model, the mass spring has lower accuracy in studying the static and dynamic behavior of the micro-beams. In order to overcome this shortcoming, in this work, the accuracy of the model has been improved using corrective coefficients. By solving the static deflection equation, the fixed points of the micro-beam are obtained for different conditions, resulting in saddle-node, pitchfork, and transcritical bifurcations. In order to study the stability of the fixed points, motion trajectories are produced in phase portraits. Moreover, dynamic response of the system to a step DC voltage also is investigated

Model Description

Figure 1a shows the schematic view of a fixed-fixed beam with length L, which is suspended between two stationary conductor plates. The beam distances from the bottom and top plates are G_1 and G_2, respectively. The illustrated beam is attracted toward the lower and upper plates by applying the voltages of V_1 and V_2, respectively. By different combination of the applied voltages and gaps, different bending states, and hence different bifurcation types, can be obtained.

In the present study, the micro-beam is assumed to be an isotropic material with modulus of elasticity E, density ρ, width b, thickness h, cross section area A and moment of inertia I.

As mentioned before, in order to simplify the analysis of the bifurcation behavior of the micro-beam, the illustrated model in Figure 1b can be simulated by an equivalent mass-spring model, which is shown in Figure 2.

Mathematical Modeling

The static deflection equation of the presented micro-switch may be computed using Euler Bernoulli beam theory. Of course the mechanical behavior the nano and micro-beams is size dependent, but as the main propose of the present paper is to study the qualitative bifurcational behavior of a micro-beam therefore the micro-beam is modeled based on classical theories. The electrostatic forces per unit length of the beam applied to the lower and upper plates can be obtained [19] as in Eqs. (1) and (2) respectively:

$$q_{elec}(V_1,\hat{w}) = \frac{b\varepsilon_0 V_1^2}{2(G_1-\hat{w})^2} \tag{1}$$

$$q_{elec}(V_2,\hat{w}') = \frac{b\varepsilon_0 V_2^2}{2(G_2-\hat{w}')^2} \tag{2}$$

Where, $\hat{W}(x)$ and $\hat{W}'(x)$ are the flexural deflection of the micro-beam with respect to the lower and upper plates, respectively. Also, $\varepsilon_0=8.854\times10^{-12}\,C^2\,N^{-1}\,m^{-2}$ is the permittivity of the vacuum within the gaps? Considering that, the deflection of the micro-beam with respect to the bottom plate equals to the negative value regarding to the upper plate, as:

$$\hat{W}=\hat{W}' \tag{3}$$

So the governing equation of the motion of the micro-beam, using Euler Bernoulli beam theorem, is:

$$EI\frac{\partial^4\hat{w}}{\partial\hat{x}^4}+\rho A\frac{\partial^2\hat{w}}{\partial t^2}=\frac{b\varepsilon_0}{2}\left(\frac{V_1^2}{(G_1-\hat{w})^2}-\frac{V_2^2}{(G_2+\hat{w})^2}\right) \tag{4}$$

Where right hand terms of this equation are resultant electrostatic forces per unit length of the beam ($q_{elec}(V_1, V_2, \hat{W})$). In Eq. (4) first and second right hand terms indicate the imposed forces from lower and upper plates, respectively.

In order to compose a lumped mass-spring model for the micro-switch, Eq. (4) is converted to Eq. (5) [4]:

$$m\frac{\partial^2\hat{y}}{\partial t^2}+K\hat{y}=\frac{b\varepsilon_0 L}{2}\left(\frac{V_1^2}{(G_1-\hat{y})^2}-\frac{V_2^2}{(G_2+\hat{y})^2}\right) \tag{5}$$

where m=ρAL is the mass of the micro-beam, and K is the spring constant for the beam and defined as the ratio of the applied uniform force 'q' to the maximum beam deflection 'Y_{max}'. Thus, the spring constant depends on the cross-section/shape of the beam as well as on the boundary conditions. Considering the mass-spring model, the

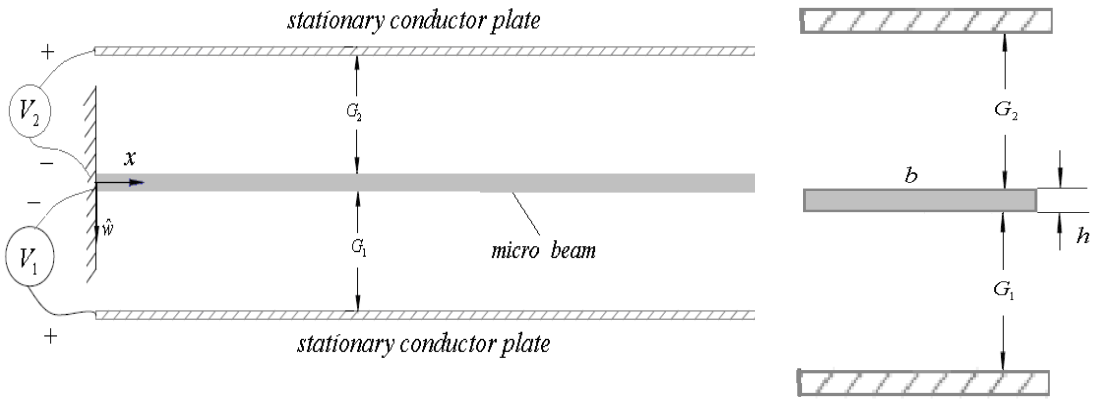

Figure 1: Schematic view of a beam-based MEM switch. a) A beam-based MEM switch; b) Cross section of the micro beam.

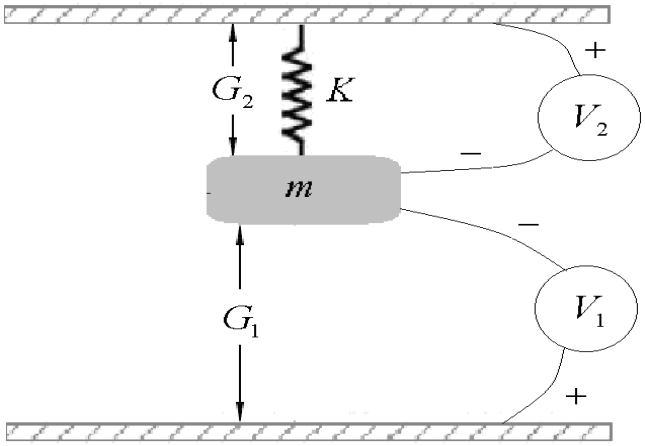

Figure 2: Mass-spring model of the micro-beam.

spring constant for cantilever and fixed-fixed beams are $8EI/L^3$ and $384EI/L^3$, respectively [4]. In order to increase the accuracy of the mass-spring model, and to adjust it with the distributed model as well, corrective coefficients of a_0 and b_0 are applied as below:

$$a_0 m\frac{\partial^2 \hat{y}}{\partial t^2}+K\hat{y}=\frac{b_0 b\varepsilon_0 L}{2}\left(\frac{V_1^2}{(G_1-\hat{y})^2}-\frac{V_2^2}{(G_2+\hat{y})^2}\right) \tag{6}$$

Where $a_0 m$ is the equivalent mass of the micro-beam. The parameters a_0 and b_0 are determined; so that the first natural frequencies and the static pull-in voltages obtained using both mass-spring and the distributed models, become equal.

For convenience Eqs. (4) and (6) can be rewritten in a non-dimensional form by defining the following parameters:

$$w=\frac{\hat{w}}{G_1},\ y=\frac{\hat{y}}{G_1},\ x=\frac{\hat{x}}{L},\ \tau=\frac{t}{t^*},\ s=\frac{G_2}{G_1},\ p=\frac{V_2}{V_1} \tag{7}$$

Where τ is the dimensionless time, and $t^*=\sqrt{\frac{a_0 m}{K}}$ for the mass-spring, and $t^*=\sqrt{\frac{\rho A L^4}{EI}}$ for the Euler-Bernoulli beam models. Therefore Eqs. (4) and (6) may be written as:

$$\frac{\partial^4 w}{\partial x^4}+\frac{\partial^2 w}{\partial \tau^2}=\alpha V_1^2\left[\frac{1}{(1-w)^2}-\frac{p^2}{(s+w)^2}\right] \tag{8}$$

$$\frac{d^2 y}{d\tau^2}+y=\alpha' V_1^2\left[\frac{1}{(1-y)^2}-\frac{p^2}{(s+y)^2}\right] \tag{9}$$

Where α and α' are the non-dimensional parameters of the electrostatic forces in the distributed and mass-spring models, respectively. These parameters are:

$$\alpha=\frac{\varepsilon_0 b L^4}{2EIG_1^3},\ \alpha'=\frac{b_0\varepsilon_0 bL}{2KG_1^3},\ (\alpha'_{\text{cantilever}}=\frac{b_0\alpha}{8}\ \alpha'_{\text{fixed-fixed}}=\frac{b_0\alpha}{384}) \tag{10}$$

Numerical Approach

Due to the presence of the nonlinear terms in Eq. (8), the analytical solution methods may not be employed to obtain the pull-in voltage '$V_{pull\text{-}in}$' of the micro-beam. Hence, the SSLM method together with Galerkin based reduced integration method are implemented to solve this equation. By using SSLM, the smooth and continuous behavior of the beam, as well as the magnitude of the nonlinear forces, can be approximated in every iteration step [13].

Static deflection

The use of static SSLM calls for smooth forces application. In the case of electrostatic forces, the voltages can be gradually increased from zero to the final value, so it satisfies the quasi-equilibrium condition.

Denoting superscript 'i' as the counting step, and w^i being the non-dimensional displacement of the micro-structure, subjected to V_1^i and V_2^i; and increasing the applied DC voltage in each step, the dimensionless static deflection at (i+1)th step can be obtained as:

$$V_1^{i+1}=V_1^i+dV_1\ \&\ V_2^{i+1}=V_2^i+dV_2\ \Rightarrow\ w^{i+1}=w^i+\delta w=w^i+\varphi^i \tag{11}$$

By considering small values for dV_1 and dV_2, the variable will be small enough; so that we can approximate the excitation function with the first two term of its Taylor series expansion in each step. As a result, Eq. (8) for the ith step and quasi-static case will be:

$$\frac{d^4 w^i}{dx^4}=q_{elect}(V_1^i,V_2^i,w^i) \tag{12}$$

and for (i+1)th step:

$$\frac{d^4 w^{i+1}}{dx^4}=q_{elect}(V_1^{i+1},V_2^{i+2},w^{i+1}) \tag{13}$$

Substituting W^{i+1}, V_1^{i+1} and V_2^{i+1} from Eq. (11) into Eq. (13) and using Taylor expansion, results in:

$$\frac{d^4 w^i}{dx^4}+\frac{d^4\phi^i}{dx^4}=q_{elec}(V_1^i,V_2^i,w^i)+\left(\frac{\partial q_{elec}}{\partial w}\Big|_{w^i}\right)\phi^i+\frac{\partial q_{elec}}{\partial V_1}dV_1+\frac{\partial q_{elec}}{\partial V_2}dV_2 \tag{14}$$

With subtracting Eq. (12) from Eq. (14) one can obtain:

$$\frac{d^4\phi^i}{dx^4}-\left(\frac{\partial q_{elec}}{\partial w}\Big|_{w^i}\right)\phi^i=+\frac{\partial q_{elec}}{\partial V_1}dV_1+\frac{\partial q_{elec}}{\partial V_2}dV_2 \tag{15}$$

This is a linear ordinary differential equation which represents the variation of the deflection along the micro-beam. This linear differential equation may be solved using Galerkin method in which φ(x) can be expressed as:

$$\phi(x)=\sum_{j=1}^{\infty}q_j\psi_j(x) \tag{16}$$

Where $\psi_j(x)$ is the jth shape function satisfying the boundary conditions of the micro-beam. The primary variable in step i "$\varphi^i(x)$" is approximated by truncating the summation series to the finite number, N:

$$\phi_N(x)\cong\sum_{j=1}^{N}q_j\psi_j(x) \tag{17}$$

By substituting Eq. (17) into Eq. (15) and multiplying them by $\psi_r(x)$ as a weight function in the Galerkin method, and integrating the outcomes from x=0 to 1, a set of algebraic equations will be generated. Solving these set of equations in each step, the deflection at any given point, under applied voltage can be determined. The pull-in voltage of the micro-beam is subsequently obtained in the last step when the instability occurs.

Dynamic analysis

For obtaining the response of the system excited by the time dependent voltage, dynamic analysis of the micro-beam has also been performed. Applying a minor modification on Eq. (4), by assuming the generalized deflections are function of time i.e.,

$$\hat{w}(x,t)=\sum_{j=1}^{N}q_j(t)\psi_j(x) \tag{18}$$

and using the Galerkin approximation method, the equation of dynamic response will be:

$$[M][\ddot{q}]+[K][q]=[F] \quad (19)$$

Where,

$$[M]_{rj}=\rho A\int_0^L \psi_j(x)\psi_r(x)dx,$$

$$[K]_{rj}=EI\int_o^L \frac{d^4\psi_j}{dx^4}\psi_r dx,$$

$$[F]_r=\int_0^L \frac{b\varepsilon_0}{2}\left(\frac{V_1^2}{(G_1-\hat{w})^2}-\frac{V_2^2}{(G_2+\hat{w})^2}\right)\psi_r(x)dx \quad (20)$$

are the effective mass, spring and actuating force matrices, respectively q(t) can be obtained from above set of ordinary differential equations (Eq. (19)) using an integration scheme.

Results and Discussion

Validation of the numerical method

The convergence of the numerical method and validation of the results may be investigated by comparing them with those given by Mobki et al. [19], and Osterberg [20]. The considered case studies in Osterberg; Medio and Lines [20,21] are fixed-fixed and cantilever micro-switches with width of 50 μm, thickness of 3 μm, Young's modulus of 169 GPa, G_1=1 μm andV_2=0V.

Bifurcation analysis

The fixed points for a fixed-fixed micro-switch with L=400 μm, G_1=3 μm, b=4 μm, h=2 μm and E= 169 Gpa has been obtained. Based on Eq. (9), physical fixed points for the micro-switch exist for –s<y<1, but mathematically, these points may also exist in the range of 1<y or y<-s. At the fixed points, the micro-beam's velocity is zero, hence considering Eq. (9), equilibrium points are obtained by solving the following equation [21]:

$$f(\alpha',s,p,y)=y(1-y)^2(s+y)^2-\alpha' V_1^2[(s+y)^2-p^2(1-y)^2]=0 \quad (21)$$

The order of polynomial in Eq. (21) is five with respect to y, having maximum five real roots. In order to check the stability in the vicinity of an equilibrium point(y=y_i), the following Jacobian matrix is used [15].

$$J=\begin{bmatrix} 0 & 1 \\ \alpha' V_1^2\left[\frac{2}{(1-y_i)^3}+\frac{2p^2}{(s+y_i)^3}\right]-1 & 0 \end{bmatrix} \quad (22)$$

Where Y_i is a fixed point. Eigen vlaues of the Jacobian satisfy $\lambda^2-\alpha V_1^2\left[\frac{2}{(1-y_i)^3}+\frac{2p^2}{(s+y_i)^3}\right]+1=0$. For λ^2<0, it has two pure imaginary roots, meaning that the fixed point (y_i, V_1) is a center point but when λ^2>0, indicating two real eigenvalues with opposite signs; which means the corresponding equilibrium point (y_i, V_1) is an unstable saddle point. Using this method, the stability in the vicinity of each equilibrium point can be identified.

Bifurcation analysis for the present micro-switch is accomplished for three different cases as following.

Geometrical symmetric micro-switch with balanced electrostatic force (P=S=1): Figure 3 depicts bifurcation diagram of a micro-beam versus applied voltage V_1 as a control parameter in the case of p=s=1. Based on the afore mentioned procedure, stability of each branch in Figure 3 can be distinguished (in this paper dashed and continues curves represent unstable and stable branches for bifurcation diagram, respectively).

In Figure 3 by increasing the control parameter V_1, three physical fixed points get closer together and for V_1=8.97V, i.e., pull-in voltage, they coalesce and change to one unstable saddle node. This condition represents subcritical pitchfork bifurcation [1], for the presented MEM switch where p=s=1.

Figures 4-7 present motion trajectories of the presented micro-switch for different values of the applied voltage V_1 with different initial conditions. As shown in Figures 4-6, in each case, there is a physical region of periodic set of center point which is bounded with heteroclinic orbit (black bold curve). Figures 4-7 show that with increasing the applied voltage, the physical region of the periodic set is contracted and when the applied voltage is equal to the pull-in voltage, this physical region of the periodic set vanishes, rendering the system unstable for any initial condition (In this paper, continues and dashed curves represent periodic and unstable orbits for phase diagrams respectively).

Geometrical non-symmetric micro-switch with balanced electrostatic force (p=s ≠ ζ; ζ ≠ 1): Bifurcation diagram of a micro-switch in the case of p=s=2 is shown in Figure 8. In the corresponding bifurcation diagram, a transcritical bifurcation occurs due to an exchange of stability between the trivial (y=0) and nontrivial branches in V_1=10.33V (primary pull-in). For this bifurcation no fixed points appear or disappear, only their stability properties change [22].

Furthermore, by increasing the controlling parameterV_1, the distance, between two nontrivial physical fixed points, is decreased and for V_1=11.04V they meet together in a saddle node bifurcation (secondary pull-in). For this case there is no physically stable branch, after pull-in voltage. But as shown in this figure, for the applied voltage10.33<V_1<11.04, there is a physically stable branch after pull-in voltage. This phenomenon can be observed in the capacitive micro-beam suspended between two conductive plates in the condition of p=s ≠1.

Figures 9 and 10 shows bifurcation diagrams for the micro-switch in the case of p=s=3 and p=s=4 respectively. As shown in these figures, the stable branches appear after primary pull-in voltage. For the case of p=s=3 and p=s=4, the mentioned branches can be observed in the ranges of 11.09<V1<13.02 and 11.49<V1<14.75 respectively. With comparison of Figures 8-10 with each other, it may be noted that with increasing of the parameter p, the mentioned stable branch is extended, for the case of p=s and G2>G1.

Figures 11-16 present motion trajectories of a micro-switch with p=s=2 (Figure 8) for different values of the applied voltageV_1, with different initial conditions. As it is seen in Figures 12 and 13, there are physical region of periodic set of center point and a region of repulsion of unstable saddle node in each diagram. It must be noted that the substrate position acts as a singular point and velocity of the system near this singular point tends to infinity. The region of periodic set of the physical center point is bounded by a bold closed orbit (homoclinic orbit). Depending on the location of the initial condition, the system can be stable or unstable. Similar to the previous case, Figures 11-13 shows that with increasing the applied voltage, the physical region of the periodic set is contracted and when the applied voltage equals to the primary pull-in voltage (Figure 14), there is no region of periodic set and the system becomes unstable for any initial conditions.

Figures 15a and 15b shows phase diagrams of the micro-switch for the case of 10.33<V_1<11.04. As shown in these figures, physical region of the periodic set exists in V_1=10.8V and disappears in V_1=11.04V (Figures 16a and 16b). This condition represents the saddle-node bifurcation in V_1=11.04V (secondary pull-in), which is shown in Figure 8.

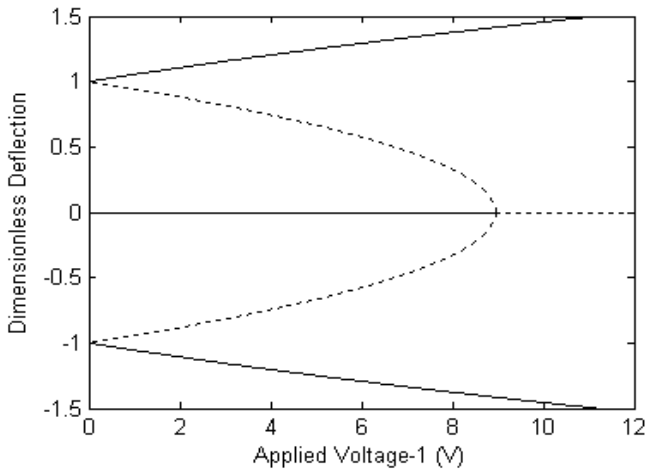

Figure 3: Equilibrium points of the micro-beam versus applied voltage (V_1) (p=s=1, $V_{pill-in}$=8.9V).

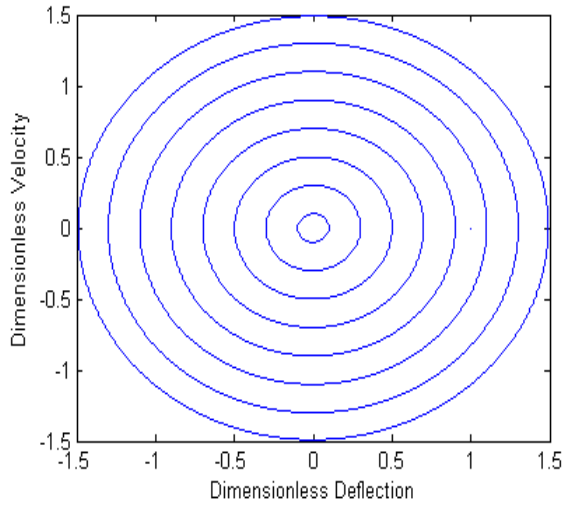

Figure 4: Phase diagram for the micro-switch when p=s=1 and V_1=0V.

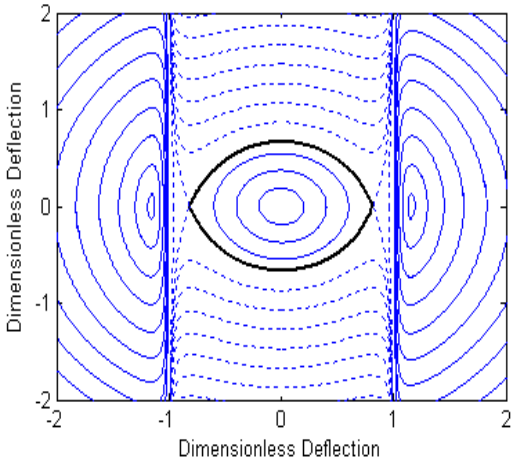

Figure 5: Phase diagram for the micro-switch when p=s=1 and V_1=3V.

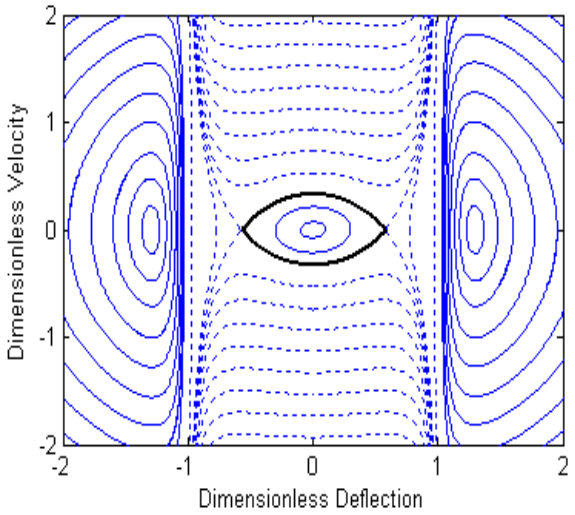

Figure 6: Phase diagram for the micro-switch when p=s=1 and V_1=6V.

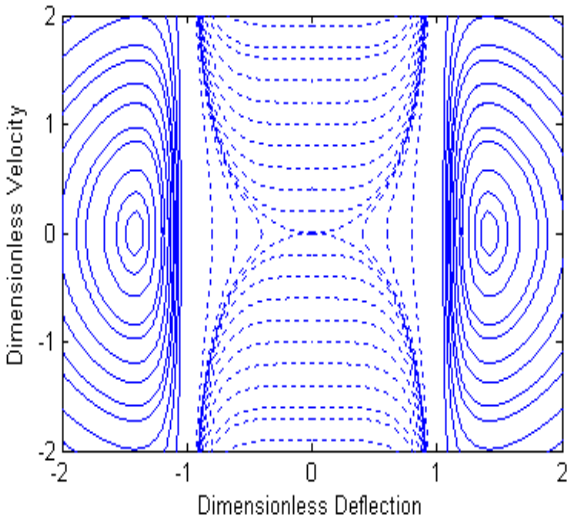

Figure 7: Phase diagram for the micro-switch when p=s=1 and V_1=8.97V.

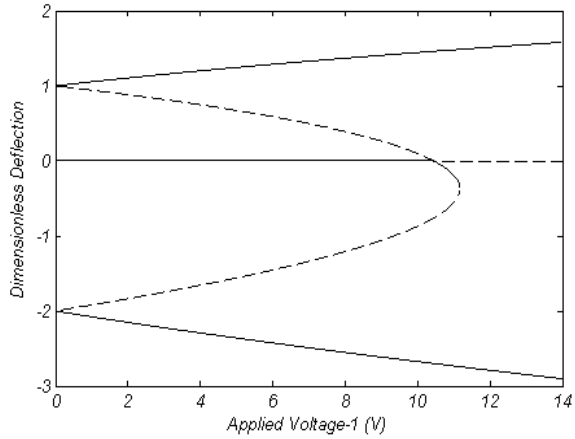

Figure 8: Equilibrium points of the micro-beam versus applied voltage V_1 (p=s=2).

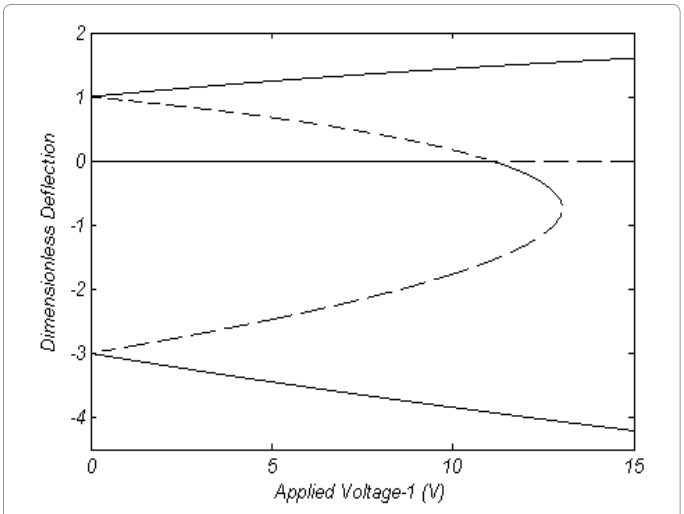

Figure 9: Equilibrium points of the micro-switch versus applied voltage V_1 (p=s=3).

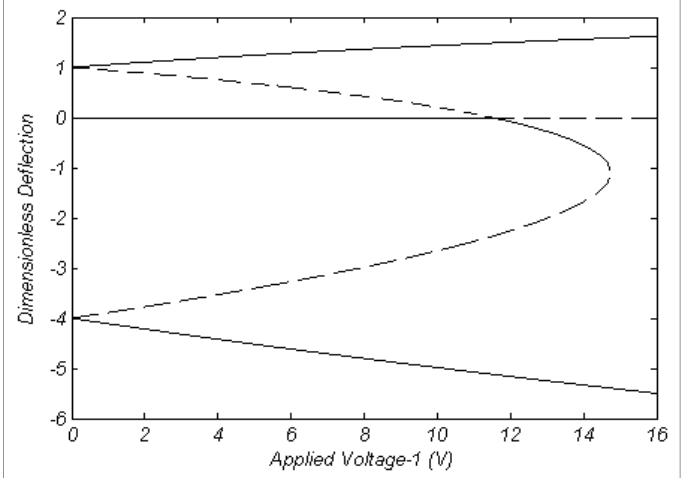

Figure 10: Equilibrium points of the micro-switch versus applied voltage V_1 (p=s=4).

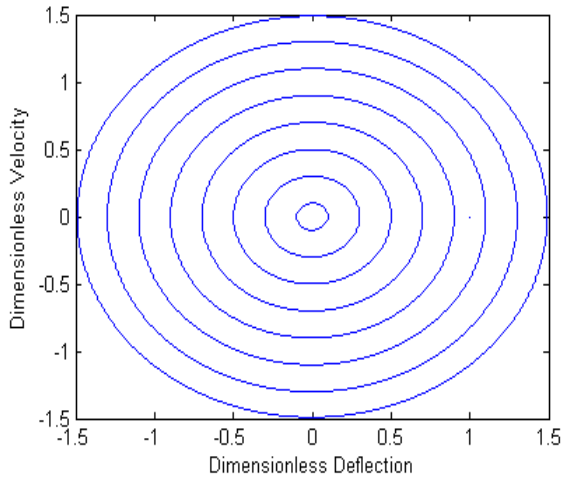

Figure 11: Phase diagram for the micro-switch when p=s=2 and V_1=0V.

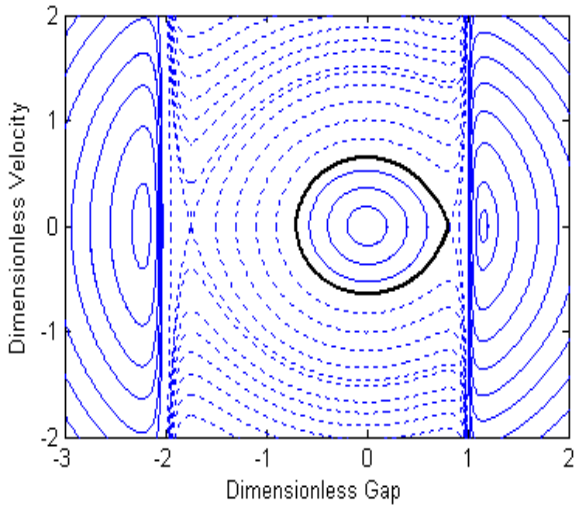

Figure 12: Phase diagram for the micro-switch when p=s=2 and V_1=3.

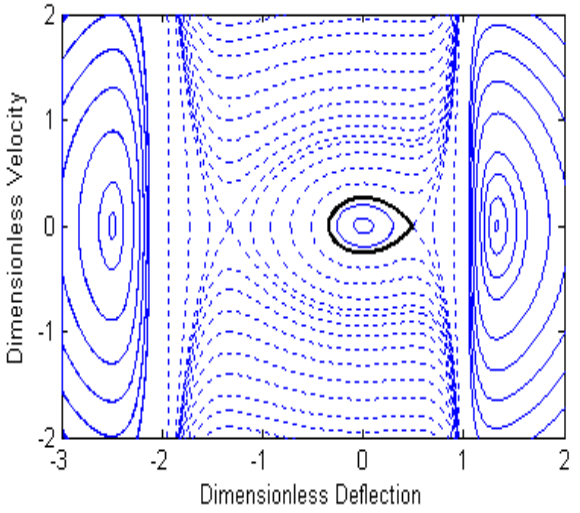

Figure 13: Phase diagram for the micro-switch when p=s=2 and V_1=7V.

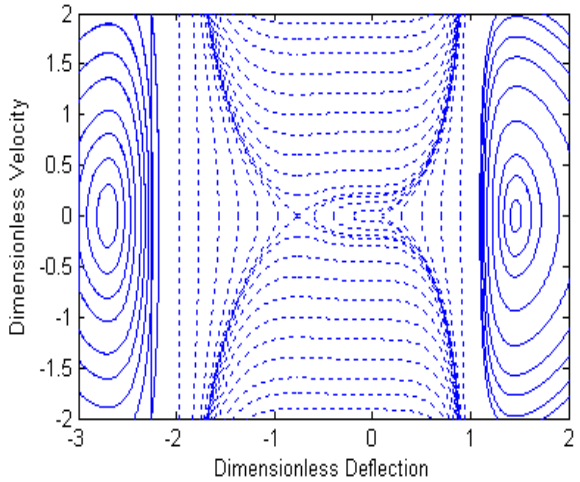

Figure 14: Phase diagram for the micro-switch when p=s=2 and V_1=10.33V.

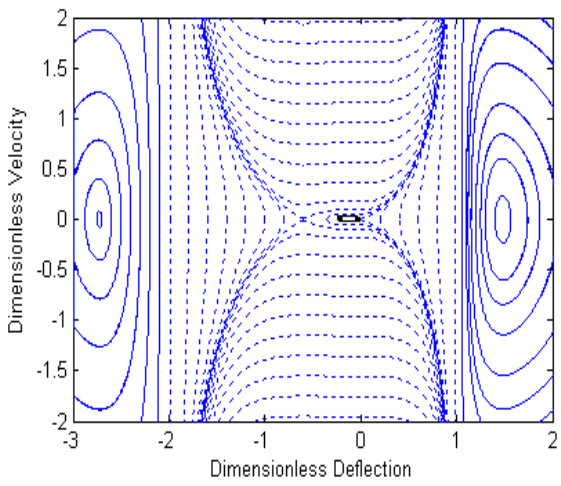

Figure 15a: Phase diagram for the micro-switch when p=s=2 and V_1=10.8V.

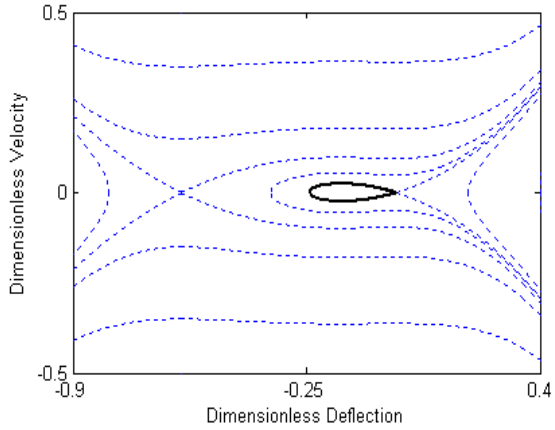

Figure 15b: A detailed closed view of the phase diagram about the fixed points when p=s=2 and V_1=10.8V.

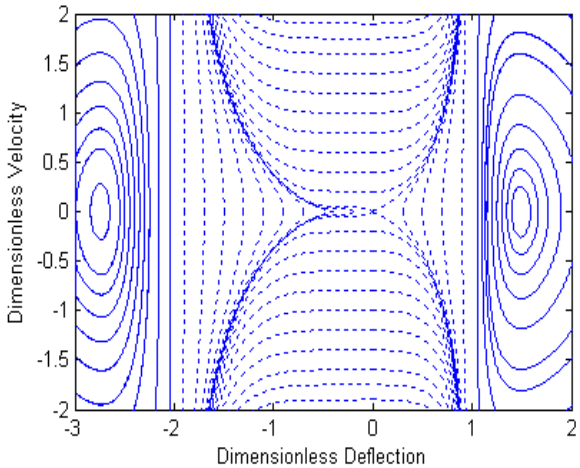

Figure 16a: Phase diagram for the micro-switch when p=s=2 and V_1=11.04V.

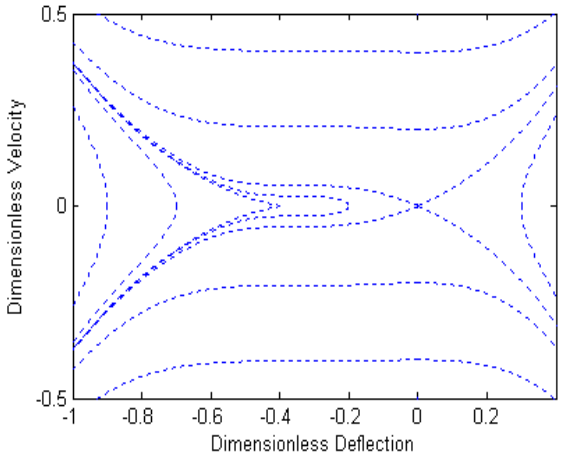

Figure 16b: A detailed closed view of the phase diagram about the fixed points when p=s=2 and V1=11.04V.

It must be noted that in the classic micro-switches the pull-in phenomenon is occurred due a saddle node bifurcation, whereas in the presented micro-switch in the symmetric case (p=s=1) the pull-in phenomenon is occurred owing to a pitch fork bifurcation and in the non-symmetric cases p=s≠1 this phenomenon is first happened primarily due to a transcritical bifurcation (can be called as primary pull-in phenomenon) and secondarily due to a saddle node bifurcation (can be called as secondary pull-in phenomenon).

In addition, it can be said that the first case p=s=1 can be obtained from the second case decreasing the value of the voltages and gap ratios (ς). With decreasing the value of (ς) the transcritical and saddle node bifurcation points approaches together and at the case when these ratios are equal to 1 (ς=1) only one saddle node bifurcation point is observed.

Geometrical non-symmetric micro-switch with un-balanced electrostatic force (p ≠ s ≠ 1): Figure 17 shows bifurcation diagram of the micro-switch in the case of $p \neq s$ (p=1, s=2). As shown in this figure, by increasing the control parameter V_1, two physical fixed points get close to each other and in V_1=7.21V, (pull-in voltage), they meet together in a saddle node bifurcation point.

Figures 18-21 shows phase diagram of the micro-switch for different values of the applied voltage V_1, with different initial conditions. As shown in Figures 18-20 there is a physical region of the periodic set of the center point in each diagram. The region is bounded by a bold closed orbit (homoclinic orbit). Depending on the location of the initial condition in the phase diagram, the system can be stable or unstable. Figures 18-21 show that with increasing the applied voltage, the physical region of the periodic set is contracted until the applied voltage reaches to the pull-in voltage; the region of the periodic set vanishes making the system unstable for any initial condition.

Dynamic response

The static bifurcation was investigated in previous subsection, and in this part we study the dynamic response of the micro-switch subjected to a step DC voltage. The solution of dynamic response is based upon Galerkin reduced order method. The physical characteristics of the studied fixed-fixed beam are L=600 μm, h=2 μm, G_1=2 μm, b=4 μm, E=169 Gpa. The static pull-in voltage for this micro-switch in the case of p=0 is 10.54 V whereas for the dynamic case is 9.62 V, which is 91.3%

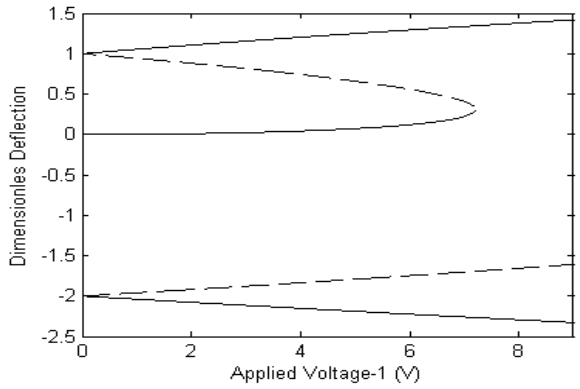

Figure 17: Equilibrium points of the micro-switch versus applied voltage V_1 (p=1, s=2, $V_{pull-in}$=7.21).

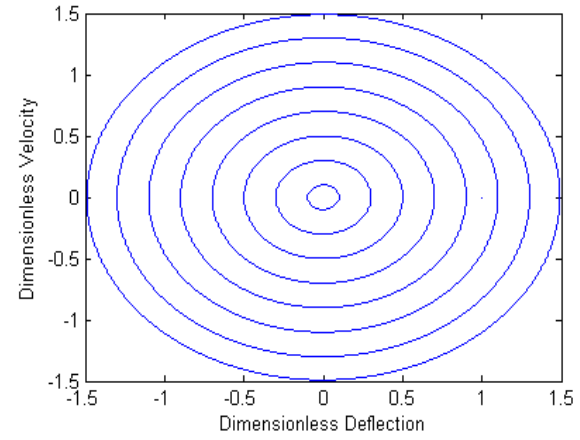

Figure 18: Phase diagram for the micro-switch when p=1, s=2 and V_1=0V.

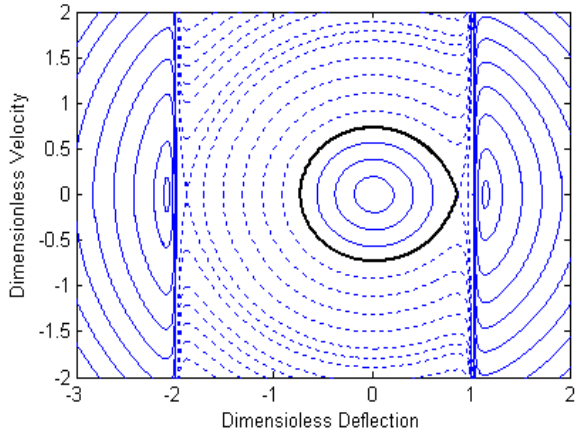

Figure 19: Phase diagram for the micro-switch when p=1, s=2 and V_1=2.5V.

of the static case. The obtained percentage is in good agreement with the reported results in Mobki et al.; Seydel [13,23]. Figure 22 shows the time history of the center deflection of the micro-beam subjected to 9.61V and 9.62V applied DC voltages, respectively. As shown in these figures, the beam is in its stable condition under 9.61V and starts to vibrate after application of this voltage, however, 9.62V applied voltage leads to instability in the mentioned beam and the dynamic pull- in phenomenon occurs.

For micro switches, with $p \neq 0$, the dynamic pull-in condition may be different from reported results [13,23]. In micro-switches with $p \neq 0$, the dynamic pull-in voltage may be equal or less than the static one. This condition occurs because of the application of two electrostatic forces with opposite directions. In addition to applied voltage, the parameter s can be effective on the dynamic response of the micro-switch.

Figure 23 shows the magnitude of dynamic pull- in voltages versus s ($1<s<10$) for p=0.5, 0.75, 1. As shown in this figure, with increasing of parameter s, for any value of p, the dynamic pull-in voltage approaches to 9.62, which agrees with the result [13,23]. On the other hand, with decreasing of the s, the dynamic pull-in voltage increases. As shown in this figure for p=1 and s=1.61 the dynamic pull-in voltage reaches to the static one. This condition for p=0.75 occurs whens=1.19. But as shown in this figure, for p=0.5 dynamic pull-in voltage is less than the static one for every magnitude of the s. for this case, maximum value of dynamic pull-in voltage is 10.07 V, which is occurred in s=1. It must be noted that the dynamic pull-in voltage cannot be more than the static one. In exact word, based on reported results of refs [13,23] and obtained results of this paper, it can be said that dynamic pull-in voltage is in the range of $0.9V_{s\text{-}pull\text{-}in} \leq V_{d\text{-}pull\text{-}in} \leq 1V_{s\text{-}pull\text{-}in}$, which $V_{s\text{-}pull\text{-}in}$ and $V_{d\text{-}pull\text{-}in}$ represent static and dynamic pull-in voltages, respectively.

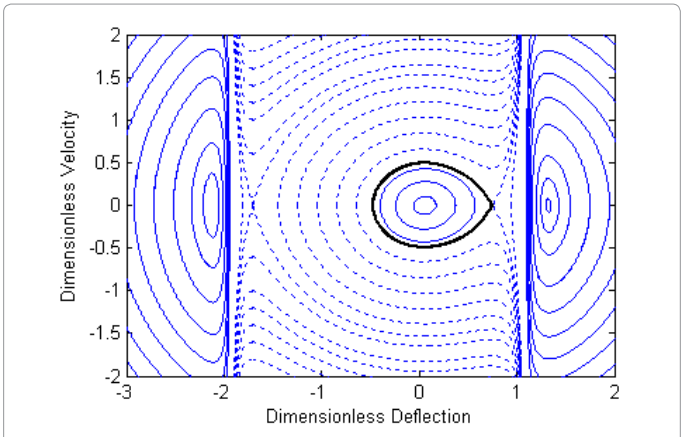

Figure 20: Phase diagram for the micro-switch when p=1 , s=2 and V_1=5V.

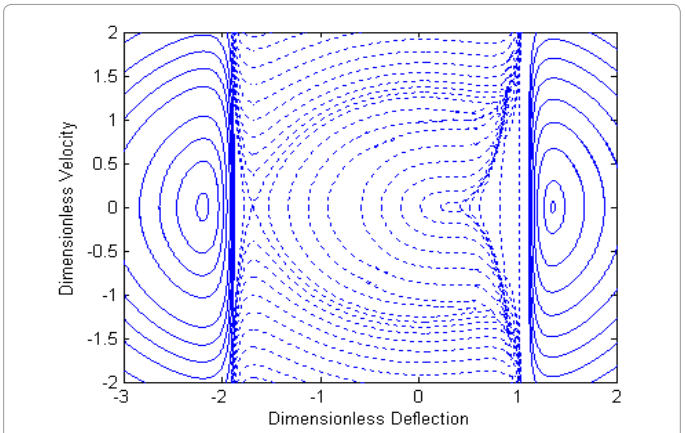

Figure 21: Phase diagram for the micro-switch when p=1, s=2 and V_1=7.2V.

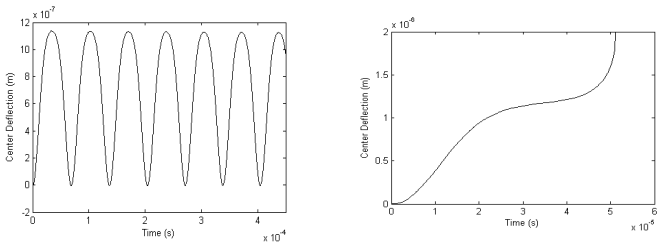

Figure 22: Dynamic response of the fixed-fixed micro-switch in the case of p=0 subjected to step-wise DC voltage. (a) Time history of the micro-beam (V=9.61V); (b) Time history of the micro-beam (V=9.62V).

So for p=1 in range of s ≤ 1 and p=0.75 in range of s ≤ 1.19, dynamic pull-in voltage is the same with static pull-in voltage.

The time history and phase portrait of the micro-beam with s=2 and p=1 and various step DC voltages is shown in Figure 24. As shown in Figure 24a the response of the micro-beam to DC voltage lower than 10.34V is periodic but for higher than this value, the response is non-periodic (unstable). This condition represents pull-in condition. As shown in this figure, with increasing of applied voltage from pull-in value, pull-in time is decreased. Figure 24b shows a metamorphosis of how a periodic orbit approaches to homoclinic orbit at dynamic pull-in voltage (V=10.34V). Indeed, the periodic orbit is ended at dynamic pull-in voltage where a homoclinic orbit is formed. In other words, when the applied voltage approaches the dynamic pull-in voltage, the periods of the closed orbits tend to infinity. It can be said that, the homoclinic bifurcation happened, when the periodic orbit collides with a saddle point at dynamic pull-in voltage. It must be noted that the scenario of instability in the case of applying step DC voltage is different from its static application. As Figure 17 shows, when applied DC voltage approaches the static pull-in voltage, the system tends to an unstable equilibrium position by undergoing to a saddle node bifurcation. A saddle node bifurcation, which is seen in the static application of the DC voltage, is a locally stationary bifurcation. This kind of bifurcation can be analyzed based on locally defined eigenvalues. In addition to local bifurcations, periodic orbits encounter phenomena that cannot be analyzed based on locally defined eigenvalues. Such phenomena are global bifurcations [24]. Furthermore for DC step excitation voltages lower than 9.2 V, the response is linear and the trajectories in the phase plane have symmetric forms. Increasing the voltage of the step excitation the trajectories in the phase plane shows a symmetric breaking for voltages between 9.2 and 10.33 V.

Conclusion

The governing equation to analyze the dynamic motion of the micro-beam suspended between two conductive plates and subjected to electrostatic forces was presented. Due to the nonlinearity of this equation, it was solved using SSLM and Galerkin weighted residual method. The bifurcation behavior of the micro-switch under various conditions and excited voltages and stationary electrodes distances from the micro-beam were obtained using a modified mass-spring model. By solving the equation of the static deflection, fixed points of the micro-switch was determined, for three different cases of p=s=1, p=s ≠ 1 and p ≠ s ≠ 1. It was shown that, the pull-in phenomena were occurred by undergoing to a pitchfork and a saddle node bifurcation in the cases of p=s=1 and p ≠ s respectively. For these cases it was shown that, there are five fixed points in range of $0<V<V_{pull\text{-}in}$, and also it was shown that this number decreases to three fixed points for $V \succ V_{pull-in}$. Also was shown that for the electro-statically balanced case p=s one of the fixed points is a trivial solution. For the case when p=s≠1it was shown that primary and secondary pull-in phenomena are observed. In this case the primary pull-in phenomenon is due to a transcritical bifurcation and the secondary one is due to a saddle node bifurcation. Furthermore it was shown that, a stable center point exists between these unstable fixed points. The length of the stable branch between these unstable fixed points is increased with simultaneously increasing

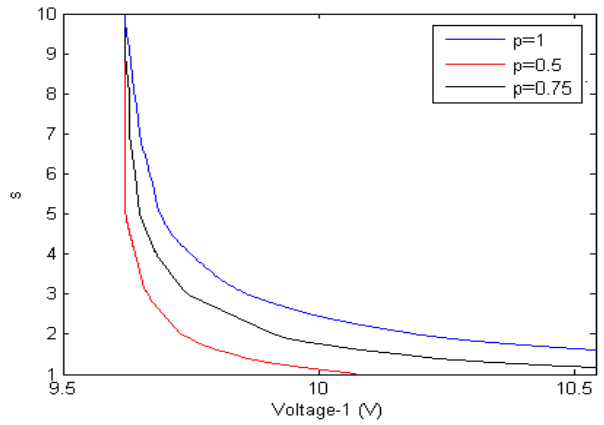

Figure 23: s vs. V_1 for the micro-switch.

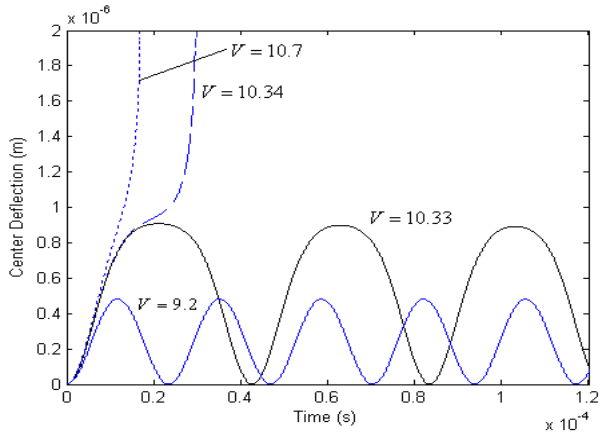

Figure 24a: Time history of the micro-switch, when s=2 and p=1.

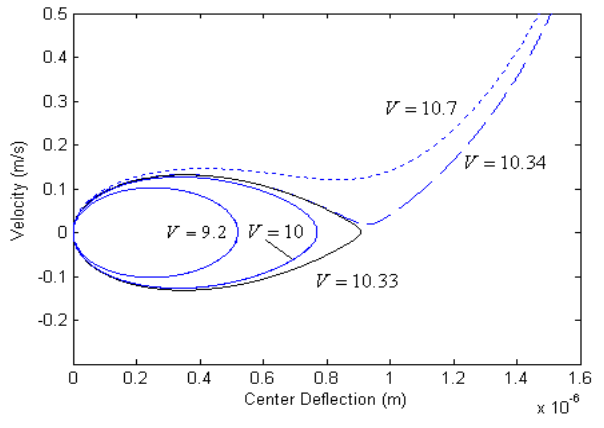

Figure 24b: Phase portrait and symmetry breaking of the micro-switch, when s=2 and p=1.

the voltages and gap ratios (ς). In another word the case of p=s=1 is a special case of the second one when these ratios are equal to 1 and in this case two bifurcation points join together and only one saddle node bifurcation is observed.

In the case of applying step DC voltage, the results show that, contrary to the classic micro-switch, for presented micro-switch, the ratio of the dynamic pull-in voltage to the static one is not a constant value and located in the range of 0.9 to 1. In another word when the system is in the electro-statically balanced case (p=s) and exist the trivial solution, as there is no inertial forces in the system, the static and dynamic pull-in values are equal.

References

1. Nayfeh AH, Balachandran B (2004) Applied Nonlinear Dynamics.
2. Rezazadeh G (2007) A comprehensive model to study nonlinear behavior of multilayered micro beam switches. Microsyst Technol 14: 135-141.
3. Zhang Y, Zhao YP (2006) Numerical and analytical study on the pull-in instability of micro-structure under electrostatic loading. J Sens Actuators A Phys 127: 366-367.
4. Lin WH, Zhao YP (2003) Dynamic behavior of Nanoscale Electrostatic actuators. Chinese Phys Lett 20: 2070-2073.
5. Arani GA, Ghaffari M, Jalivand A, Kolahchi R (2013) Nonlinear nonlocal pull-in instability of boron nitride nanoswitches. Acta Mech 224: 3005-3019.
6. Jia LX, Yang J, Kitipornchai S (2011) Pull-in instability of geometrically nonlinear micro-switches under electrostatic and Casimir forces. Acta Mech 218: 161-174.
7. Mobki H, Rezazadeh G, Sadeghi M, Vakili-Tahami F, Seyyed-Fakhrabadi MM (2013) A comprehensive study of stability in an electro-statically actuated micro-beam. Int J Nonlinear Mech 48: 78-85.
8. Zhang Y, Zhao YP (2006) Numerical and analytical study on the pull-in instability of micro-structure under electrostatic loading. Sensors and Actuators A 127: 366-380.
9. Taghizadeh M, Mobki H (2014) Bifurcation analysis of torsional micromirror actuated by electrostatic forces. Arch Mech 66: 95-111.
10. Dequesnes M, Tang Z, Aluru NR (2004) Static and Dynamic Analysis of Carbon Nanotube-Based Switches. J Eng Mater-T Asme 126: 230-237.
11. Dequesnes M, Rotkin SV, Aluru NR (2002) Calculation of pull-in voltages for carbon-nanotube-based nanoelectromechanical switches. Nanotechnology 13: 120-131.
12. Hosseini M, Sadeghi-Goughari M, Atashipour SA, Eftekhari M (2014) Vibration analysis of single-walled carbon nanotubes conveying nanoflow embedded in a viscoelastic medium using modified nonlocal beam model. Arch Mech 66.
13. Mobki H, Sadeghi MH, Rezazadeh G, Fathalilou M, Keyvani-janbahan AA (2014) Nonlinear behavior of a nano-scale beam considering length scale-parameter. Appl Math Model 38: 881-1895.
14. Lin WH, Zhao YP (2005) Casimir effect on the pull-in parameters of nanometer switches. Microsyst Technol 11: 80-85.
15. Lin WH, Zhao YP (2005) Nonlinear behavior for nanoscale electrostatic actuators with Casimir force. Chaos Soliton Fract 23: 1777-1785.
16. Lin WH, Zhao YP (2007) Stability and bifurcation behavior of electrostatic torsional NEMS varactor influence by dispersion forces. J Phys D Appl Phys 40: 1649-1654.
17. Shabani R, Sharafkhani N, Tariverdilo S, Rezazadeh G (2013) Dynamic analysis of an electrostatically actuated circular micro-plate interacting with compressible fluid. Acta Mech 224: 2025-2035.
18. Sharafkhani N, Rezazadeh G, Shabani R (2012) Study of mechanical behavior of circular FGM micro-plates under nonlinear electrostatic and mechanical shock loadings. Acta Mech 223: 579-591.
19. Mobki H, Rashvand K, Afrang S, Sadegh MH, Rezazadeh G (2014) Design, Simulation and Bifurcation Analysis of a Novel Micromachined Tunable Capacitor with Extended Tunability. T Can Soc Mech Eng 38: 15-29.
20. Osterberg P (1995) Electrostatically actuated microelectromechanical test structures for material property measurement. Ph.D. thesis, MIT, Cambridge, USA.
21. Medio A, Lines M (2003) Nonlinear Dynamics A Primer. Cambridge University Press, England.
22. Ananthasuresh GK, Gupta RK, Senturia SD (1996) An approach to macromodeling of MEMS for nonlinear dynamic simulation. In: Proceedings of the ASME International Conference of Mechanical Engineering Congress and Exposition (MEMS). Atlanta, GA, pp: 401-407.
23. Seydel R (2010) Practical Bifurcation and Stability Analysis. In: Verlag S (ed.) NY, USA.
24. Kuznetsov YA (1997) Elements of Applied Bifurcation Theory (2nd edn.). In: Verlag S (ed.) NY, USA.